

CERN-TH.7436/94
hep-ph/9409249

ANOMALOUS EVOLUTION OF NONSINGLET STRUCTURE FUNCTIONS

Stefano Forte* and Richard D. Ball†

*Theory Division, CERN
CH-1211 Genève 23, Switzerland*

Abstract

We review a formalism that includes the effects of nonperturbative U(1) symmetry breaking on the QCD evolution of nonsinglet structure functions. We show that a strong scale dependence is generated in an intermediate energy range $0.5 \lesssim Q^2 \lesssim 5 \text{ GeV}^2$ for all values of x . We show that this explains naturally the observed violation of the Gottfried sum, and allows a determination of the shape of the nonsinglet structure function, in excellent agreement with experiment. We argue that these effects may affect the determination of α_s from deep-inelastic scattering.

*Presented at QCD '94
Montpellier, France, June 1994*

To be published in the proceedings

CERN-TH.7436/94
September 1994

* On leave from INFN, Sezione di Torino, Turin, Italy

† On leave from a Royal Society University Research Fellowship

Accurate measurements of nonsinglet nucleon structure functions have been accomplished only rather recently. Because gluons decouple from nonsinglet quantities, such measurements provide a direct handle on the quark structure of the nucleon, and their scale dependence can be reliably calculated in perturbative QCD. In particular, the first moment of the nonsinglet nucleon structure function $F_2^{\text{NS}} = F_2^p - F_2^n$ has been determined rather accurately[1]:

$$S_G \equiv \int \frac{dx}{x} F_2^{\text{NS}} = 0.235 \pm 0.026. \quad (1)$$

This experimental result* is somewhat puzzling in view of the interpretation of F_2^{NS} and its first moment S_G in the QCD parton model: in the DIS scheme to all orders

$$F_2(x) = x \sum_i e_i^2 (q_i(x) + \bar{q}_i(x)), \quad (2)$$

where $q_i(x)$ are the distribution of quarks of flavor i in the given target, so that, using isospin,

$$F_2^{\text{NS}} = \frac{x}{3} (u^p(x) + \bar{u}^p(x)) - (d^p(x) + \bar{d}^p(x)), \quad (3)$$

where u^p and d^p are up and down quark distributions in the proton. Now, S_G is to leading order scale independent; hence at all scales S_G would be expected to be close to its quark model value, obtained assuming the quark distributions in Eq.(3) to be given by valence quarks: this, however, leads to $S_G = \frac{1}{3}$.

A possible interpretation of this discrepancy is that isospin is broken; however, isospin violation in this channel is [4] at least one order of magnitude smaller than required to explain Eq.(1). Thus the data (if correct) imply that it is the identification of the quark distributions in Eq.(3) with valence distributions to fail: the sea must have a large nonsinglet component, anticorrelated to the valence. It is easy to reproduce this sort of scenario in effective models of the nucleon[4]. However, due to the (one-loop) scale independence of S_G , such a nonsinglet component cannot be generated perturbatively from the starting valence distributions.

*Very recent data[2] show evidence for shadowing in scattering on deuterium. If this effect is confirmed the value Eq.(1) should be reduced by a further 10–15 %

The evolution equation for nonsinglet quark distributions takes the simple general form[3]

$$\frac{d}{dt} [q \pm \bar{q}] = (\mathcal{Q}_{qq} \pm \mathcal{Q}_{q\bar{q}}) \otimes [q \pm \bar{q}], \quad (4)$$

to any perturbative order, where

$$q = u - d; \quad \mathcal{Q}_{qq} \equiv \mathcal{P}_{qq}^D - \mathcal{P}_{qq}^{ND}, \quad (5)$$

and \mathcal{P}^D (\mathcal{P}^{ND}) is any quark–quark splitting function $\mathcal{P}_{q_i q_j}$ such that $i = j$ ($i \neq j$). At one loop, the only process which leads to nonsinglet evolution is gluon radiation (Fig.1a), which contributes to \mathcal{P}_{qq}^D but has vanishing first moment. This conservation holds true to all orders in the charge-conjugation odd case, but fails beyond leading order in the C-even one. Two-loop evolution is then driven by the diagram of Fig.1b: whereas the flavor-invariance of QCD leads one to expect that this should contribute equally to \mathcal{P}^D and \mathcal{P}^{ND} , due to Fermi statistics the final state must be antisymmetrized with respect to the two identical quarks when $i = j$, while this is not the case if $i \neq j$. This is enough [5] to lead to nonvanishing values for all the nonsinglet anomalous dimensions, which, however, remain very small.

In QCD, axial $U(N_f)$ flavor symmetry is broken down to $SU(N_f)$ by non-perturbative effects due to the axial anomaly. This leads to a large difference between flavor-preserving and flavor-changing transitions[6], and thus to sizable values of the anomalous dimensions[7]. Indeed, assume that the emitted and unobserved $q\bar{q}$ pair may form a bound state (Fig.1c). Emission of neutral (charged) mesons will then contribute to \mathcal{P}_{qq}^D (\mathcal{P}_{qq}^{ND}). In the pseudoscalar sector, where $U(1)$ symmetry breaking manifests itself, π^\pm emission will thus contribute to \mathcal{P}_{qq}^{ND} , and π^0 and η emission to \mathcal{P}_{qq}^D (considering for simplicity the $SU(2)$ case). Because of the much larger mass of the η the flavor-preserving process is suppressed, thus leading to a large negative value for \mathcal{Q}_{qq} . This leads to sizable evolution, with the sign required to explain the result Eq.(1).

This argument can be made quantitative [7] by setting up generalized evolution equations which include an effective coupling to bound states of the form of Fig.1c. Because symmetry breaking only appears in the Goldstone sector, only pseudoscalar mesons need to be included. Introducing a nonsinglet pion distribution $\pi \equiv \pi^+ - \pi^-$, the nonsinglet evolution equations

are then

$$\frac{d}{dt}q = \mathcal{Q}_{qq} \otimes q + \mathcal{Q}_{q\bar{q}} \otimes \bar{q} + \mathcal{P}_{q\pi} \otimes \pi, \quad (6)$$

$$\frac{d}{dt}\bar{q} = \mathcal{Q}_{q\bar{q}} \otimes \bar{q} + \mathcal{Q}_{qq} \otimes q - \mathcal{P}_{q\pi} \otimes \pi, \quad (7)$$

$$\frac{d}{dt}\pi = \mathcal{P}_{\pi q} \otimes (q - \bar{q}) + \mathcal{P}_{\pi\pi} \otimes \pi. \quad (8)$$

It is still necessary to specify the effective quark-meson coupling, denoted by a blob in Fig.1c. The total cross section for the process of Fig.1c turns out to depend [7] only on a pseudoscalar and an axial vertex function; the former dominates for intermediate values of Q^2 (up to a few GeV^2), while the latter controls the large Q^2 tail. As a consequence, the bulk of the splitting function depends on one single parameter Λ , the radius of the form factor, which is related by the chiral Ward identity to the constituent quark mass M_q . The large Q^2 tail depends also on the axial coupling g_π , which is expected to be $g_\pi \lesssim \frac{1}{2}$.

It may now be checked explicitly that \mathcal{P}_{qq} can be computed in the LLA, in that the cross section is dominated by a collinear singularity where the coupling is effectively pointlike. The anomalous dimensions are sizable for values of Q^2 up to 5–10 GeV^2 , while at both very small $Q^2 \sim 0.05 \text{ GeV}^2$, and at large $Q^2 > 10 \text{ GeV}^2$, all the anomalous dimensions flatten, ensuring smooth connection to a valence quark picture in the infrared and to the usual perturbative behaviour in the ultraviolet. As expected, \mathcal{P}^{ND} is larger than \mathcal{P}^{SD} by roughly a factor two, thus leading to significant nonsinglet evolution.

The scale dependence of S_G can now be determined: the result obtained assuming S_G to take the “quark model” value $S_G = 1/3$ at a reference scale $Q_0 \sim 200 \text{ MeV}$ is shown in Fig.2 as a function of the two parameters M_q and g_π , and compared to the experimental result. Very good agreement is obtained with reasonable values of the parameters. This means that the full nonsinglet sea is generated dynamically: therefore, not only its first moment but its full shape can now be predicted[8].

To this purpose, we need a model for the starting valence and its evolution at low scale. Once this is specified[9], the nonsinglet structure function is fully

determined at all x and Q^2 , because the bulk of the low- Q^2 nonperturbative effects is expected to be encapsulated by the anomalous evolution equations (6–8). The scale dependence is driven by two competing mechanisms: gluon radiation (Fig.1a) which softens the valence quark distribution, and bound state emission (Fig.1c) which leads to a net increase in the number of sea $q-\bar{q}$ pairs. Thus, the peak of the nonsinglet distribution as a function of x remains approximately fixed at its starting value $x \sim \frac{1}{3}$, rather than shifting towards smaller x as it happens in the singlet case. However, the overall decrease of the structure function is stronger than found with ordinary perturbative evolution.

The structure function determined thus is compared to the data[†] and to the result of ordinary perturbative evolution in Fig.3. It is apparent that the effects of anomalous evolution are large for all values of x . The (unphysical) effect of switching gluon emission off is also shown. In the large- x region, where the NMC data have large errors, an alternative comparison can be made with more precise data at a larger value of Q^2 [11]. The stability of these results upon variation of the parameters has been checked explicitly [8].

Drell-Yan scattering can provide a direct determination of

$$R(x) \equiv \frac{\bar{d}(x) - \bar{u}(x)}{\bar{d}(x) + \bar{u}(x)}. \quad (9)$$

Predicting the value of $R(x)$ in the anomalous evolution scenario would require a computation of singlet evolution as well; we may however estimate it by assuming the bulk of the effect of anomalous evolution on the singlet to be just the production of an asymmetric sea. The result (Fig.4) has the generic feature of saturating to a constant when $x \gtrsim 0.2$ because at large x the symmetric sea vanishes more rapidly than the anomalously generated asymmetric one (as discussed above), thus only the latter contribution to R survives, which is just equal to a constant group-theoretic factor. Our result is in excellent agreement with the data [12, 13], which however cannot exclude some of the alternative models; a measurement of R Eq.(9) for several values of x would be required to discriminate between them.

[†]Notice that the data have been recently revised; the new data agree better with our prediction [8] than those [10] to which we originally [8] compared it.

The scale dependence of the full nucleon structure function F_2^p is dominated by nonsinglet evolution if $x \gtrsim 0.3$ because the gluon distribution falls very rapidly at large x . Thus, anomalous evolution will affect the scale dependence of F_2^p at large x and intermediate values of Q^2 . We may estimate this effect by again assuming that the bulk of the anomalous contribution to both singlet and nonsinglet is just due to the diagram of Fig.1c. Then, in this range of x and Q^2 F_2^p will decrease less rapidly as a function of $\log Q^2$ than it would if anomalous evolution were neglected, essentially because of the anomalous production of $q\bar{q}$ pairs discussed above, which counters the softening of the structure function (Fig.5a). Of course, at large Q^2 the usual results are regained.

A decrease of $|d \ln F_2^p / d \ln Q^2|$ of the same size is found if $\alpha_s(M_z)$ is reduced by roughly 10 % (Fig5b, from Ref.[15]). Because the value of α_s is extracted [15] from F_2 by fitting its scale dependence while neglecting anomalous evolution, if the effect is indeed present the value of α_s is systematically underestimated. Of course the relevant fits include also the small- Q^2 region, where higher-twist effects are dominant, and the large- Q^2 region, where anomalous evolution is negligible; a new global fit is thus required to pin down the size of the effect. The sign of the effect and order of magnitude, however, appear to be just what required in order to bring this determination of α_s in line with the LEP value.

Acknowledgements: Part of the work described here was done in collaboration with V. Barone and M. Genovese. We thank G. Altarelli for pointing out the relevance of our results to the determination of α_s , and M. Arneodo and C. Quigg for discussions.

References

- [1] M. Arneodo et al. (NMC), Phys. Rev. D50 (1994) 1
- [2] B. Badełek and J. Kwieciński, Phys. Rev. D50 (1994) 4; see also B. Badełek, these proc.
- [3] G. Altarelli, Phys. Rep. 81 (1982) 1
- [4] S. Forte, Phys. Rev. D47, (1993) 1842
- [5] D. A. Ross, C. T. Sachrajda, Nucl. Phys. 149 (1979) 497
- [6] E. J. Eichten, I. Hinchliffe and C. Quigg, Phys. Rev. D45 (1992) 2269
- [7] R. D. Ball and S. Forte, Nucl. Phys. B, in press. See also S. Forte, Acta Phys. Pol. B25 (1994) 159
- [8] R. D. Ball, V. Barone, S. Forte and M. Genovese, Phys. Lett. B329 (1994) 505
- [9] V. Barone et al., Zeit. Phys. C58 (1993) 541
- [10] P. Amaudruz et al. (NMC), CERN preprint PPE/93-117 (1993), unpublished
- [11] A. Benvenuti et al. (BCDMS), Phys. Lett. B223 (485) 1989
- [12] P. L. McGaughey et al. (E772), Phys. Rev. Lett. 69 (1992) 1726
- [13] A. Baldit et al. (NA51), Phys. Lett. B332 (1994) 244
- [14] S. Kumano and J. T. Londergan, Phys. Rev. D44 (1991) 717
- [15] M. Virchaux and A. Milsztajn, Phys. Lett. B274 (1992) 221

Figure Captions

Fig. [1] Diagrams which contribute to \mathcal{P}_{qq} : a) perturbative one loop; b) perturbative two loops; c) one loop bound-state emission

Fig. [2] Anomalous evolution of S_G (Eq.1) for various values of the constituent quark mass M_q (a) and of the axial coupling g_π (b).

Fig. [3] Comparison of the nonsinglet structure function generated dynamically by gluon and bound state emission with the data[1]. The results obtained switching off gluon emission or bound state emission are also shown.

Fig. [4] Comparison of the experimental results for the SU(2) antiquark asymmetry R (Eq.9) with the prediction of various models.

Fig. [5] Change in the scale dependence of the structure function F_2 due to the inclusion of nonsinglet anomalous evolution effects (a) or variation of the value of α_s (b, from Ref.[15]).

This figure "fig1-1.png" is available in "png" format from:

<http://arxiv.org/ps/hep-ph/9409249v3>

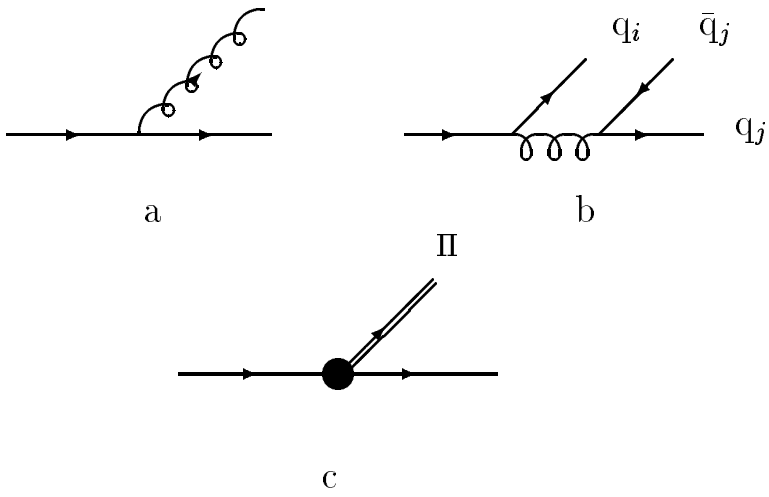
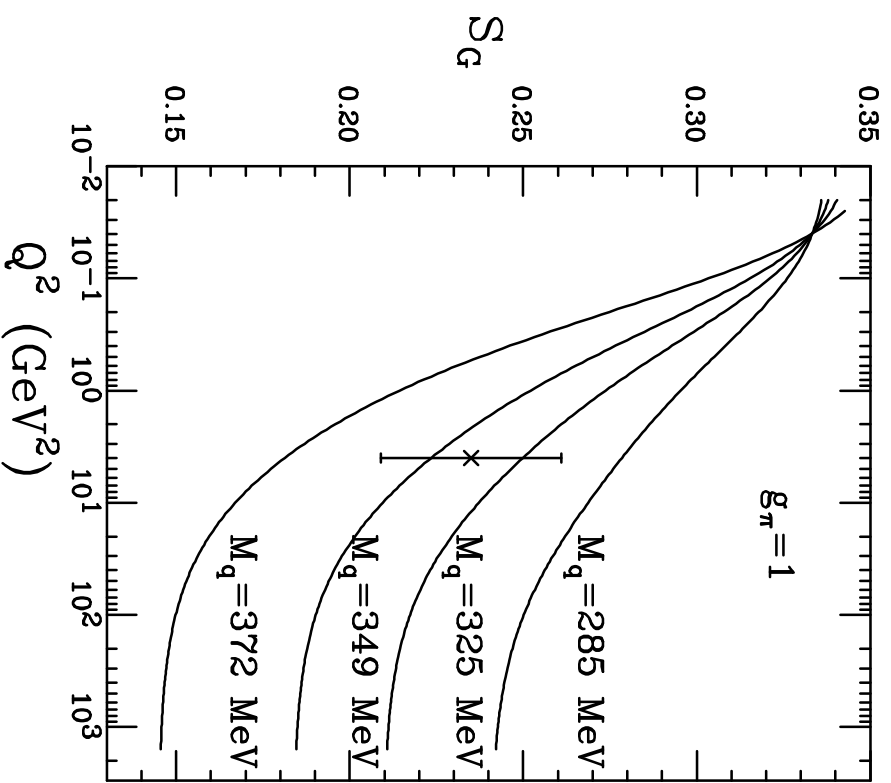


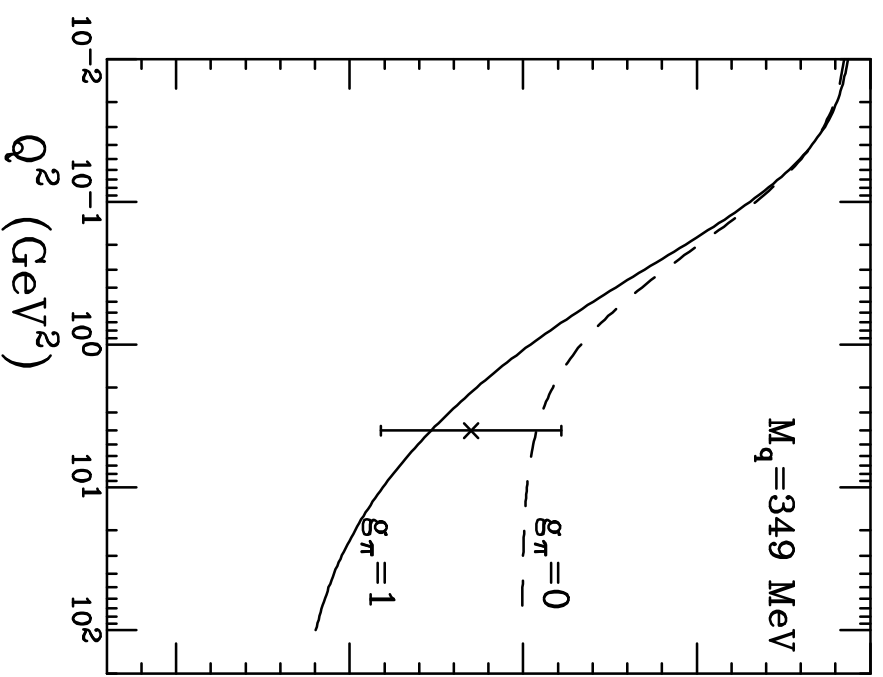
Fig. 1

This figure "fig1-2.png" is available in "png" format from:

<http://arxiv.org/ps/hep-ph/9409249v3>



a



b

Fig. 2

This figure "fig1-3.png" is available in "png" format from:

<http://arxiv.org/ps/hep-ph/9409249v3>

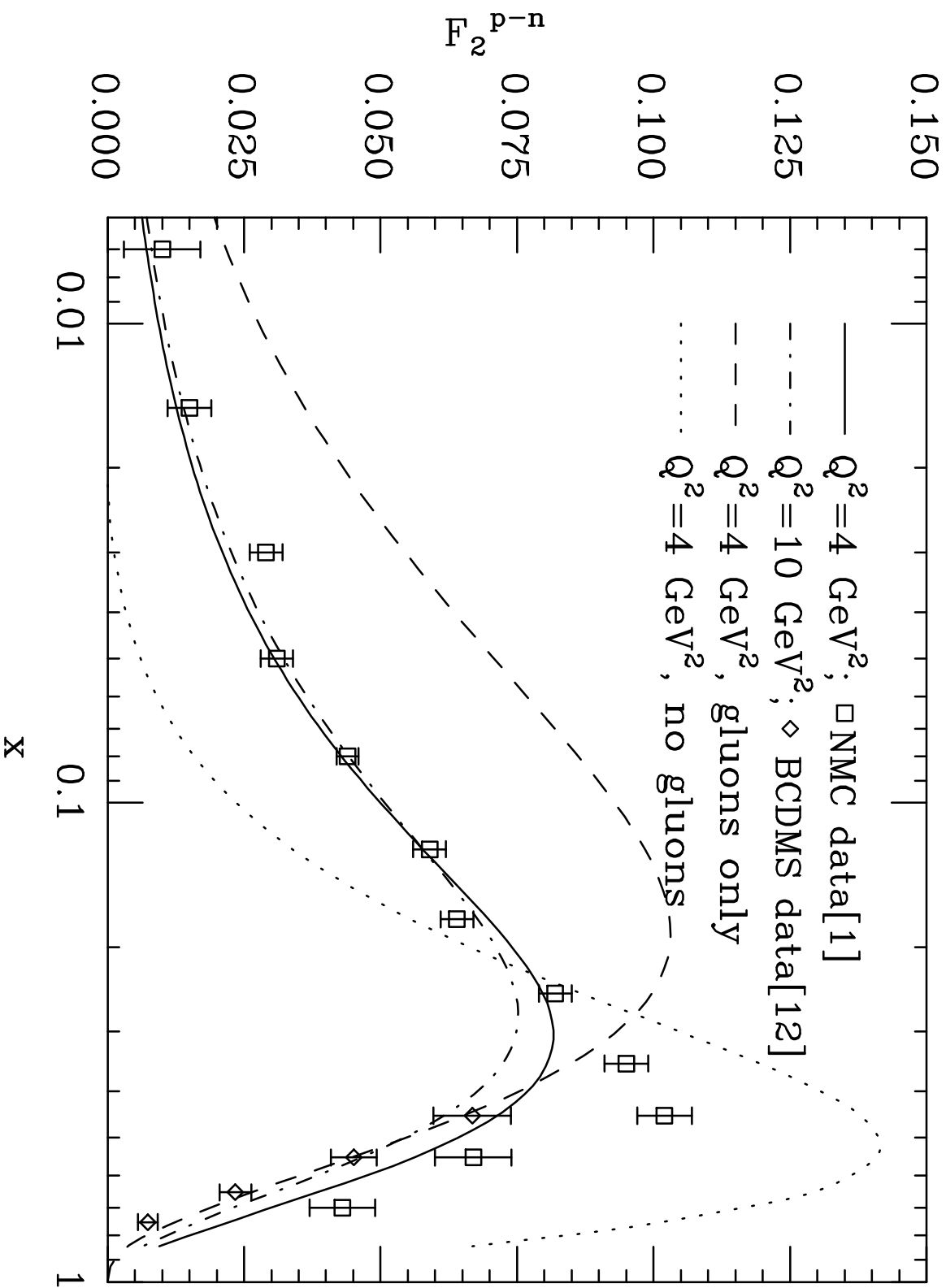


Fig. 3

This figure "fig1-4.png" is available in "png" format from:

<http://arxiv.org/ps/hep-ph/9409249v3>

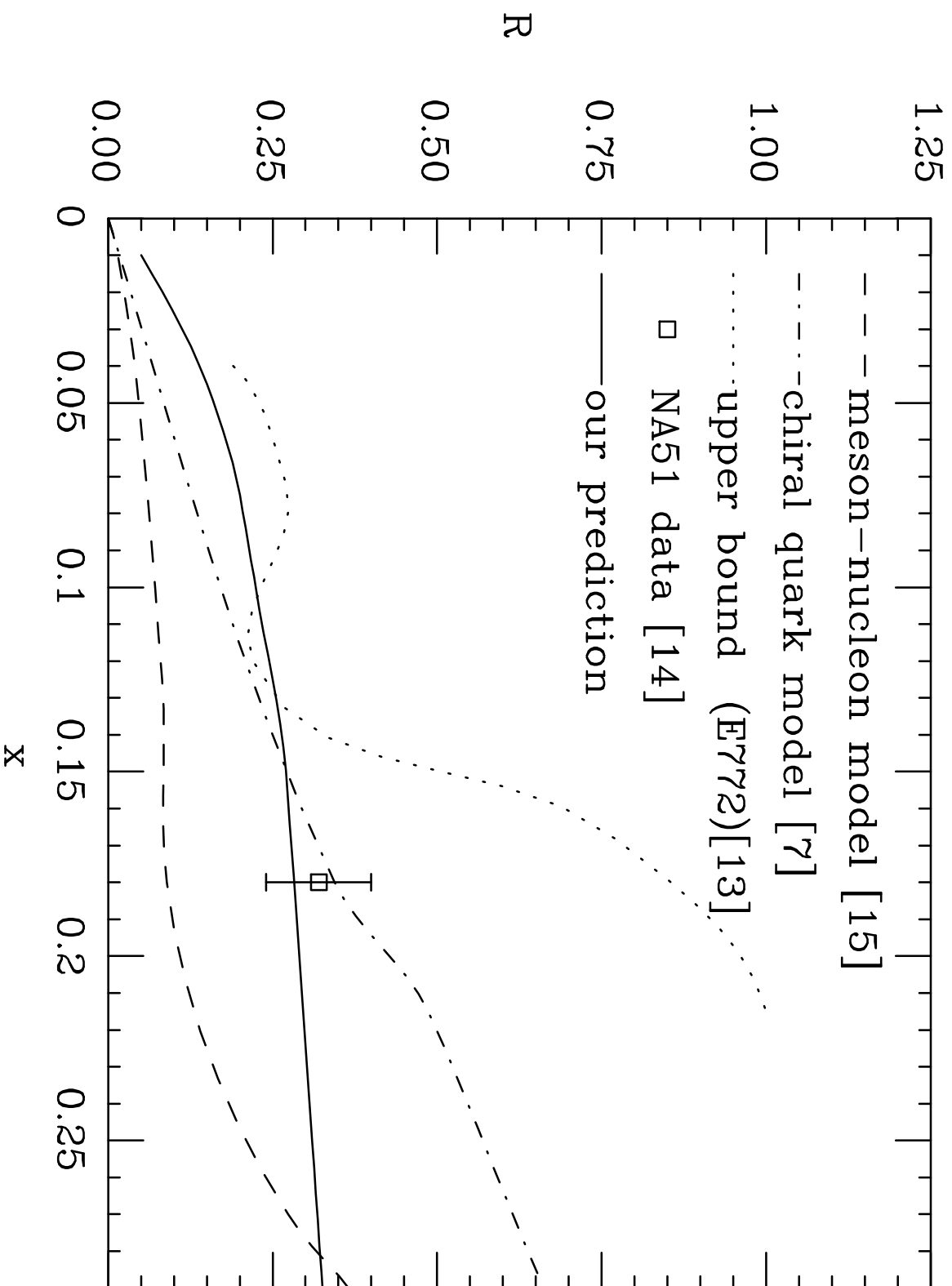


Fig. 4

This figure "fig1-5.png" is available in "png" format from:

<http://arxiv.org/ps/hep-ph/9409249v3>

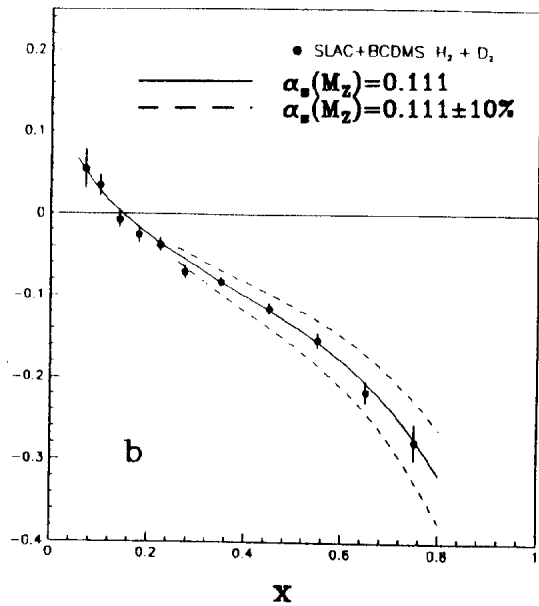
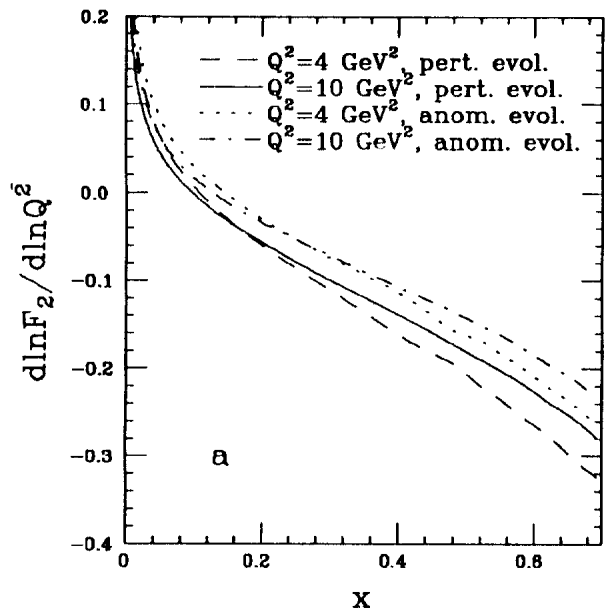


Fig. 5